

Conceptual Model of Suswa Geothermal Prospect, Kenya

Jill Robinson Haizlip, William Cumming, Nicholas Hinz, Glenn Melosh, Keg Alexander, Mark Harvey, Runar Magnusson and Sunna Björg Reynisdóttir

Geologica Geothermal Group Inc, 5 Third Street Suite 420, San Francisco, CA 94103

jhaizlip@geologica.net

Keywords: Suswa, Kenya, East African Rift, conceptual model, gas geochemistry, MT, well target

ABSTRACT

Geothermal conceptual models for the Suswa Geothermal Prospect have been developed to support resource assessment and well targeting based on the integration of previous geoscience studies with new geologic, geochemical and geophysical field surveys conducted in 2016 by EFLA and GDC scientists supported by ICEIDA and the Nordic Development Fund. The new field studies include fumarole steam and gas sampling, a CO₂ flux survey, geology and structure mapping, MT-TEM resistivity surveys and a gravity survey. The favored conceptual model derived from the integrated analysis of these data includes a magmatically-heated, 250 to 300°C, neutral, low-gas, partially two-phase reservoir associated with hot volcanic rock overlying recent intrusions that may include magma at 2.5 to 5 km depth within the Suswa inner caldera. However, the configuration and parameters of a geothermal resource at Suswa are relatively uncertain due to challenging field conditions that resulted in ambiguous results from many fumarole gas analyses and a lack of MT-TEM coverage in the inner caldera that precluded the detection of a shallow low resistivity zone corresponding to the clay cap characteristic of analogous geothermal fields. Alternate conceptual models have been developed to accommodate the related uncertainty. Despite the presence of numerous fumaroles between the inner caldera and the north wall of the outer caldera, the preferred and pessimistic conceptual models exclude this area because the gas geochemistry and resistivity pattern are consistent with a ~100°C steam zone outflowing along tuff-lava contacts near the water table at about 600 m depth and leaking to the surface along fault traces. Shallow ~100°C steam outflow also likely extends to the south, exemplified by the numerous steam vents leaking from porous tuffs exposed in the inner caldera wall. Conceptual issues encountered in other Kenyan geothermal fields that may also limit the capacity of a Suswa reservoir include the possibility of cold meteoric down flow through recent eruption vents that may depress the top of a high temperature reservoir and the possibility that shallow magma may result in a shallow base of a reservoir. On the other hand, the optimistic model assumes that evidence of magmatism below most of the inner caldera implies heating of a large overlying ~300°C resource that outflows at >250°C to the north at 2 km depth and possibly continuing to an intermediate depth below the northern outer caldera boundary. Within the overall context of the conceptual models, the key elements that most affect the risk assessment of targets at Suswa are the fumaroles with 250 to 300°C geothermometry located over intersections of structures likely to form open space permeability at reservoir depths.

1. INTRODUCTION

Mount Suswa, located about 50 km west of Nairobi, is the southernmost of the quaternary shield volcanos in the Eastern Rift Valley of Kenya (Figure 1). The numerous fumaroles found in the nested calderas had made Suswa a subject for many geothermal research projects. In 2015, the Icelandic International Development Agency (ICEIDA) and the Nordic Development Fund supported a Suswa Volcano Geothermal Project that included geothermal exploration surveys and analyses directed at developing geothermal resource conceptual models to support resource assessment and well targeting. To complete the project, EFLA Engineers (EFLA) was contracted to manage a team of subconsultants from Geologica Geothermal Group, Cumming Geoscience, Glenn Melosh, and Harvey Geoscience who performed field work, data analysis and interpretation with technical geoscience and logistics support from the staff of the Geothermal Development Company (GDC) in Kenya.

The Suswa volcano morphology is characterized by two nested calderas, a roughly circular outer caldera of about 10 km diameter and a younger inner caldera of about 5 km diameter with a central uplifted 2.5 by 3.5 km block known as the Central Island surrounded by a volcanic (water-less) moat. Numerous thermal manifestations are found in both the inner and outer caldera, including fumaroles, altered ground and areas of grass species characteristic of geothermal systems in the Kenyan Rift. Fumaroles are associated with the caldera rims, structural intersections with the caldera rims, structural alignments across the outer caldera floor, and porous tuffs exposed in the inner caldera wall. Because of the deep water table, there are no hot springs at Suswa.

Previous geoscientific studies that are relevant to the geothermal exploration at Suswa included geological mapping by McCall et al. (1965), and detailed petrologic studies, geological mapping, and major and trace element studies by numerous researchers including Johnson (1969), Nash et al. (1969), Skilling (1988 and 1993), Randel and Johnson (1970), Omenda (1993) and Macdonald et al. (1993).

Existing geochemistry of surface manifestations included fumaroles samples collected and analyzed in 1986-1987 by Iceland GeoSurvey (ISOR; Ármannsson, 1987), and samples collected and analyzed by GDC in 2012 to 2013 (Lagat and Malimo, 2013; Sekento and Kipngok, 2013). Although both steam + gas and liquid (steam condensate) samples were collected and analyzed, the steam condensate chemistry did not support much interpretation beyond the conclusion that the water does not contain reservoir brine. Previous results of the geochemical evaluation of Suswa indicated that the source of the fumaroles was geothermal steam with estimated reservoir temperatures between 230 and 280°C.

In 1999 KenGen conducted geophysical exploration at the prospect and in 2012-2013 GDC expanded those surveys by collecting magnetotelluric (MT) and transient electromagnetic (TEM) soundings in Suswa. In 2013, Mohamud (2013) presented a 1D joint

resistivity inversion results based on these sounding pairs, and Lagat and Malimo (2013) presented a geothermal model of Suswa based on the integration of geophysical surveys, including earthquake, MT-TEM resistivity and gravity data, with geochemistry and geological interpretations. The results indicate that a geothermal system exists in Suswa with magma chamber beneath the volcano acting as a heat source and a reservoir temperature estimate based on gas geothermometry of about 300°C.

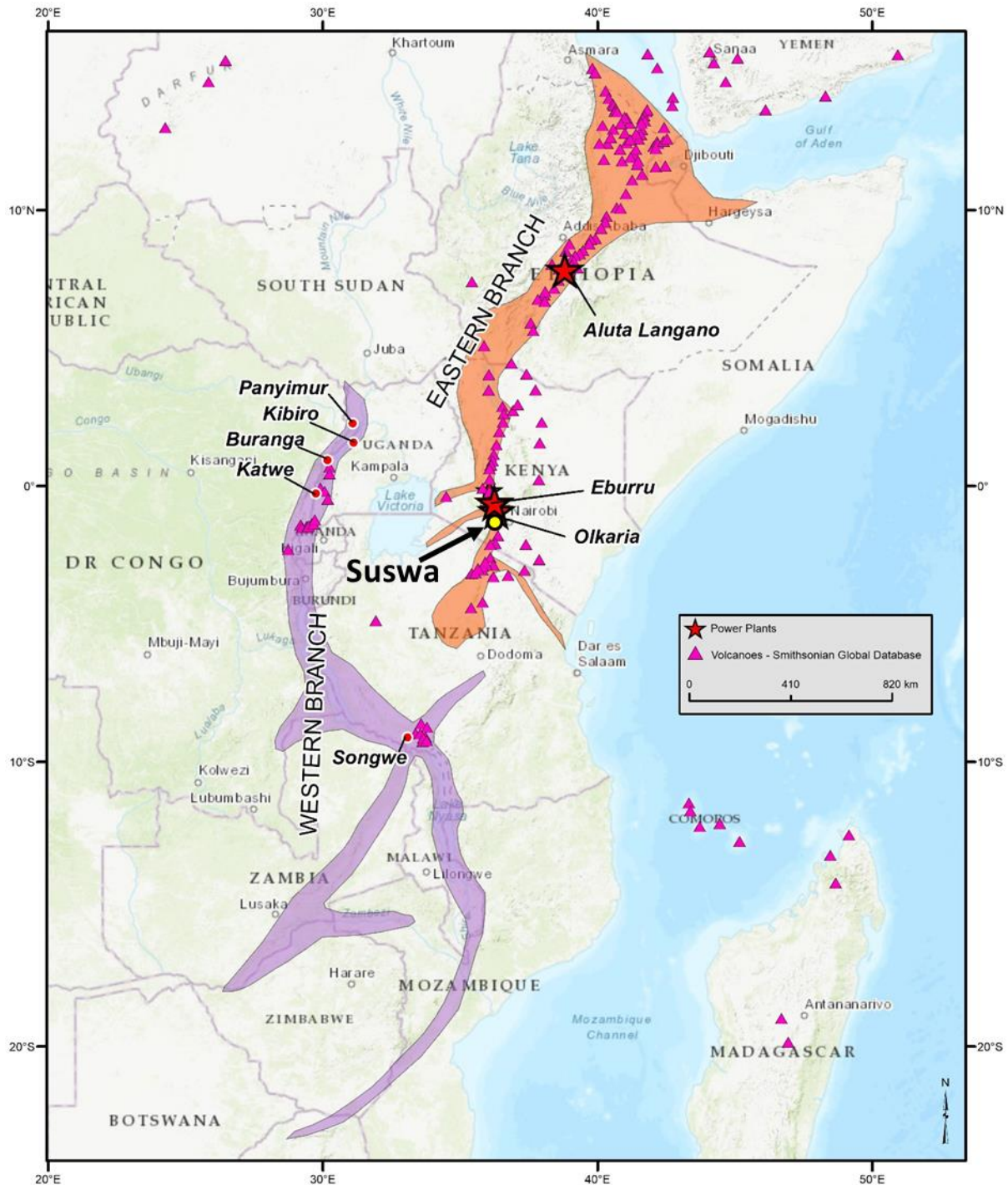


Figure 1: Location of Suswa relative to the East African Rift System (EARS).

1.1 Geologic Setting

Tectonism and volcanism associated with the Kenyan rift segment of the East African Rift System (EARS) initiated about 23 Ma. Major rifting developed from 11 to 5 Ma amidst ongoing volcanism and led to the development of the complex arrays of normal, oblique-slip, and strike-slip faults that are visible across the floor of the Kenyan rift valley (Chorowicz, 2005). The Suswa volcano started building about 0.4 to 0.2 Ma and sits on top of about 3 km of Neogene volcanic and sedimentary rocks that in turn overlie Precambrian basement (Achauer et al., 1992). Based on gravity and earthquake results, the Suswa region of the Kenyan rift also marks the southernmost extent of asthenosphere intrusion into the axis of this rift (Bonavia et al., 1995). Through modeling InSAR elevation changes centered on Suswa, Biggs et al. (2009) concluded that magma is probably locally present at 2.5 to 4 km depth under the surface of the Suswa caldera system (Figure 2).

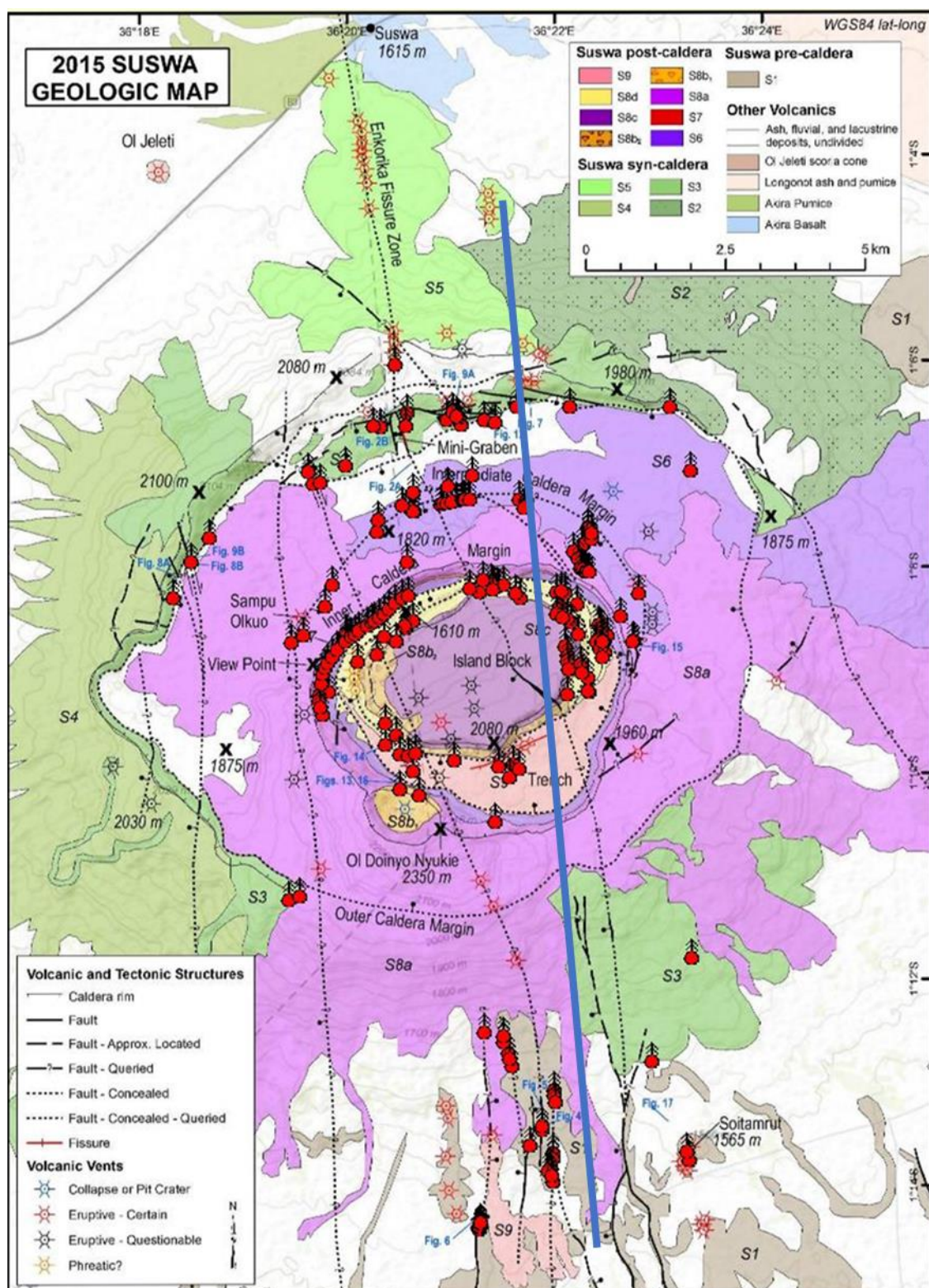


Figure 2: 2015 Suswa Geologic Map (from Hinz, 2017) – Rift fault-caldera fault interactions and stratigraphy control fumarole occurrence (fumaroles shown by symbols). The bold blue line shows the N-S cross-section that appears in Figure 10.

The regional fault kinematics have changed with the evolution of the EARS. Initially, the extension direction across the Kenyan rift was oriented northeast-southwest. This extension direction rotated to approximately east-west by early Quaternary time and has further rotated to northwest-southeast during the late middle Quaternary (Strecker et al., 1990; Bosworth et al., 1992; Smith and Mosely, 1993; Chorowicz et al., 1994; Atmaoui and Hollnack, 2003). This has implications for the range of structures that have evolved through time for this part of the rift and for the permeability patterns present today, both in Suswa and pre-Suswa stratigraphy that may be part of this geothermal system.

2. KEY RESULTS FROM FIELD STUDIES

2.1 Geological Mapping

The field geology study initially relied on two geothermal geology studies of Suswa, one by the United Nations from 1984-1989 (e.g., Torfason, 1987) and another by the former Kenya Power Company (e.g., KPC; 1993). In addition to these geothermal studies, many volcanology and petrology studies have been conducted from the 1960s through recent years (e.g., Johnson, 1969; Nash, 1969; Baker et al., 1988; Skilling, 1993; Espejel-Garcia, 2009; White et al., 2012) and regional studies of the stratigraphic framework, structural evolution, and modern day stress-strain fields have also been published in peer-review journal articles (e.g., Strecker et al., 1990; Delvaux and Barth, 2010). Both Torfason (1987) and KPC (1993) briefly discussed the potential roll of structures on permeability and the distribution of geothermal activity. However, previous studies have not focused on collecting geomechanical data for Suswa, only for the surrounding parts of the rift valley, and thus the local stress field and kinematics of faults directly associated with Suswa have not previously been studied.

Stratigraphy on Suswa Volcano includes a series of tuffs and lavas deposited over the last 240 ka overlying relatively uniform trachyte lavas that built the original shield volcano, and which was intruded by dikes and sills. The volcano is noted for having two main calderas, the primary (outer) caldera is 10 to 12 km in diameter and the inner caldera is about 5 km across (Figure 2). The caldera complex has accommodated at least 400 to 500 m of subsidence. Geologic cross-sections constructed in this study indicate that the Suswa volcanic pile ranges from about 350 to 500 m-thick outside of the outer caldera, 500 to 1000 m-thick between the outer and inner calderas, and at least 1000 to 1200 m-thick inside the inner caldera. One lava flow covers more than half of the floor of the inner caldera moat and issued from an east-northeast-striking fissure along the south side of the island block (Figure 2). A phonolite lava flow that erupted from a north-south oriented fissure on the south flank of Suswa has been interpreted to be the youngest erupted material from Suswa, possibly <1000 years old.

Suswa has two volcano-tectonic axes defined by fault and vent alignments associated with the volcanic edifice. The primary volcano-tectonic axis is oriented north-northwest and the secondary axis is oriented east-northeast. The primary axis is similar to adjacent volcanic centers, including the northwest-trending axis at Longonot and north-trending axis for Olkaria (BGS, 1990). Fieldwork in 2015 confirmed that the current stress field is associated with NW-SE extension, yielding dextral and dextral oblique motion on rift-parallel structures (EFLA, 2016). The second axis is parallel to transform accommodation zones that transect this rift segment. These volcano-tectonic axes probably result from pre-Quaternary volcano rift structures that have continued to coevolve with each volcanic center, guiding volcanic vent locations, fault propagation, and fault kinematics.

The geology and structure at Suswa reported by the EFLA team (EFLA, 2016; Hinz, 2017) integrated previous studies with more field observations and detailed analysis of current patterns of strain. In summary, a regional clockwise rotation of maximum extension from NE-SW to NW-SE has occurred. Local stresses at Suswa are complex. In addition to rifting, local stress variations have been related to episodic magmatic activity as well as possible stress transfer across Suswa Volcano in a pattern that might result in development of a right-stepping extensional step-over between right lateral-normal oblique master faults to the SW and NE of the volcano. These complex stresses lead to a variety of structural patterns in the prospect.

Rift fault patterns at Suswa generally show strong, subparallel, roughly NNW trends (Figure 2). Two main rift faults are interpreted to cut across the calderas (Figures 3 and 4). A more complex set of faults near these two is mapped south of the volcano. The caldera faults include the outer and inner caldera ring faults, a ring fault around the Island Block, and intermediate caldera ring faults expressed in the northern moat of the outer caldera. A reversal of ring fault movement during subsidence and resurgence developed a complex ring fault zone around the Island Block. These two main fault patterns, tectonic and magmatic, are complicated by secondary splays and local crossing faults associated with secondary strains. Caldera rim stresses may be partly analogous to weakly filled hole in a rigid plate as suggested by various studies. This would result in compressive circumferential stress concentrations immediately outside the caldera rim.

Field mapping and analysis at Suswa identified numerous fault complications and intersection which could produce permeability (EFLA, 2016; Hinz, 2017). An example of a hot permeable altered locked fault irregularity occurs at the southeast edge of the Island Block (Figure 3). In this area a rift axis fault intersects the Island Block ring fault. A local NW-striking fault segment radiating from the intersection cuts the south edge of the Block. (The geologic map shows a continuation of the rift fault through a bend along this segment). The interpreted right lateral sense of motion on the rift fault would put this segment in compression. A series of landslide scarps trend north from the intersection. These surface failures are on an extensional fracture trend and show abundant sulfurous alteration and fumaroles that produce reservoir type gases. Because of the deep connection evident from the fumarole chemistry, the landslides are assumed to obscure underlying extensional or oblique faults or an extension of the curving ring fault zone. Another parallel local fracture without landslide offset may cut the island block west of the landslides as evident from aligned alteration in the ASTER image (Figure 3). The complex north-trending extensional feature, its interaction with the ring fault zone in the inner caldera moat, and possible influence of the intermediate caldera ring fault to the north supports an interpretation of associated fracture permeability at reservoir depth.

A rift fault-ring fault zone intersection occurs on the northern edge of the inner caldera (also in Figure 3). Fumarole activity in the SE extensional quadrant of the intersection, at SWF 20, has high geothermometry, suggesting a correlation of this structure with deep permeability.

Another intersection example can be found in the SW inner caldera at the complex intersections of another rift axis fault and the inner caldera and Island Block ring faults (Figure 4). This intersection on the caldera ring fault is associated with alteration and fumarole activity to the west. The intersection with the Island Block ring fault just to the north shows fumarole activity in the NW, extensional quadrant. The complexity of the ring fault zone and the intersection is consistent with an interpretation of extensional permeability in either direction along the ring fault zones.

In addition to the mapping, enhancement of ASTER data using classification based on known alteration in the inner caldera was performed to identify alteration in areas with difficult access (Figure 5).

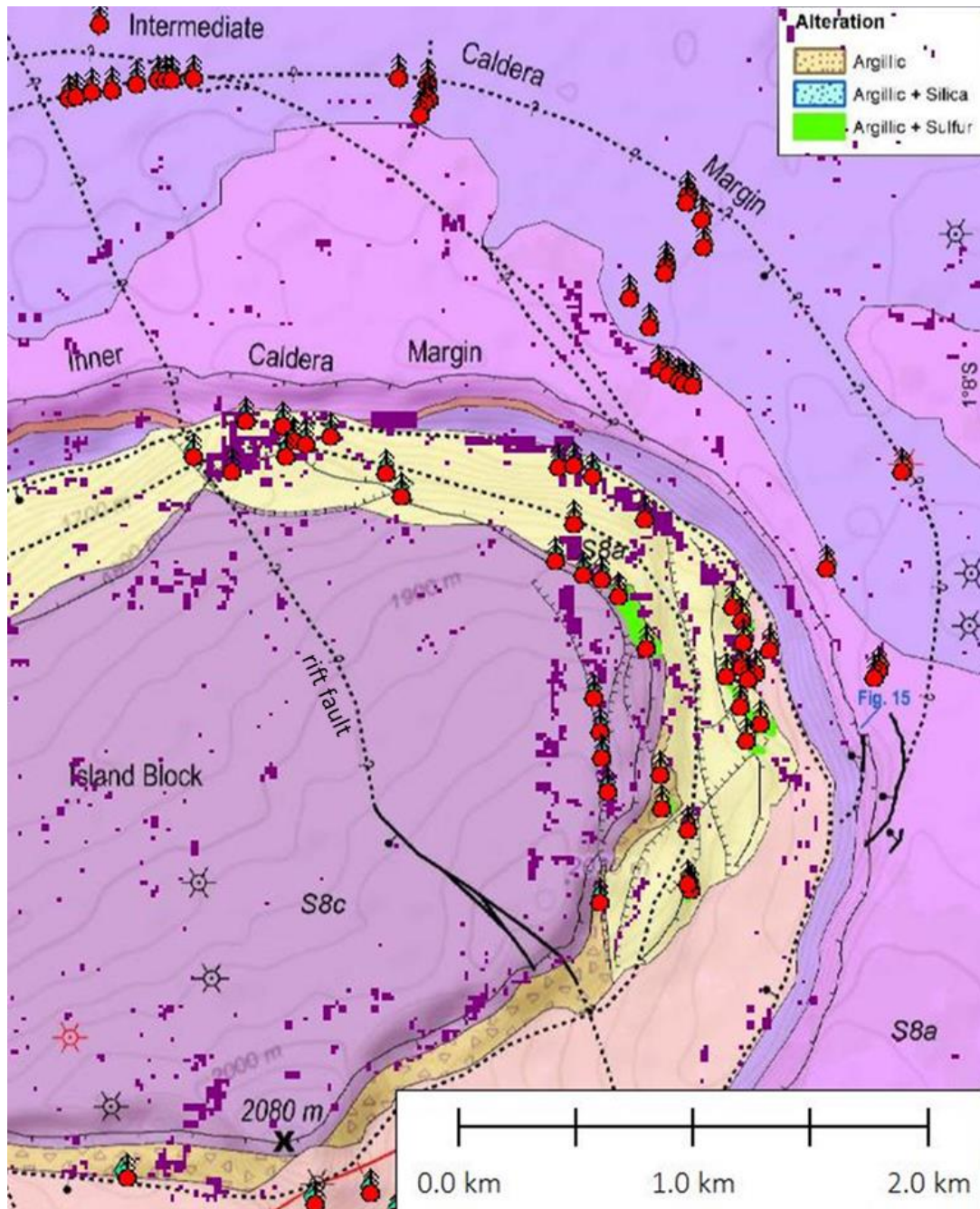
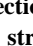


Figure 3: Suswa Geology, Alteration, and Fumaroles (from EFLA, 2016) – Landslide scarps on the east edge of the Island Block near a restraining bend in the rift fault may overlie extension in the ring fault zone. An ASTER alteration lineament (in purple) occurs on an extensional fault trend west of the landslides. A rift – ring fault intersection on the northern inner caldera rim shows fumaroles (symbols ) north of the eastern inner caldera. A NW-SE striking rift fault is labeled, which exhibits observed normal and inferred dextral offset.

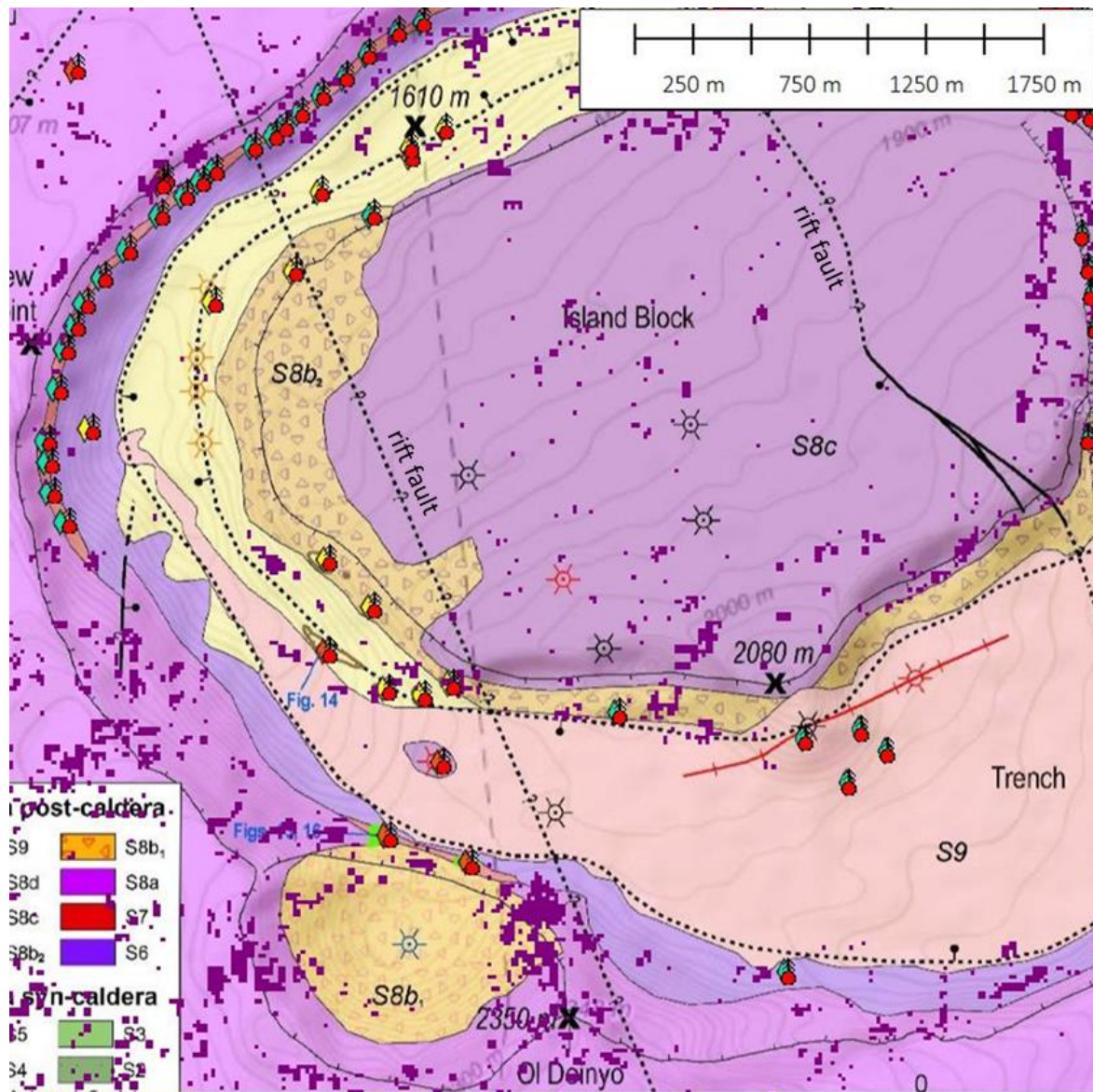


Figure 4: Western inner caldera Geology, Alteration, and Fumaroles (from Hinz, 2017) – Intersections of the western rift fault and inner caldera ring faults show alteration and fumarolic activity near the intersection. ASTER alteration is shown in purple. Fumaroles on the NW inner caldera rim align with the S7 tuff and show the impressive stratigraphic control in the lava tuff sequence. The complete legend for the geologic base map is shown in Figure 2. Two NW-SE striking rift faults are labeled, which exhibit observed normal and inferred dextral offset.

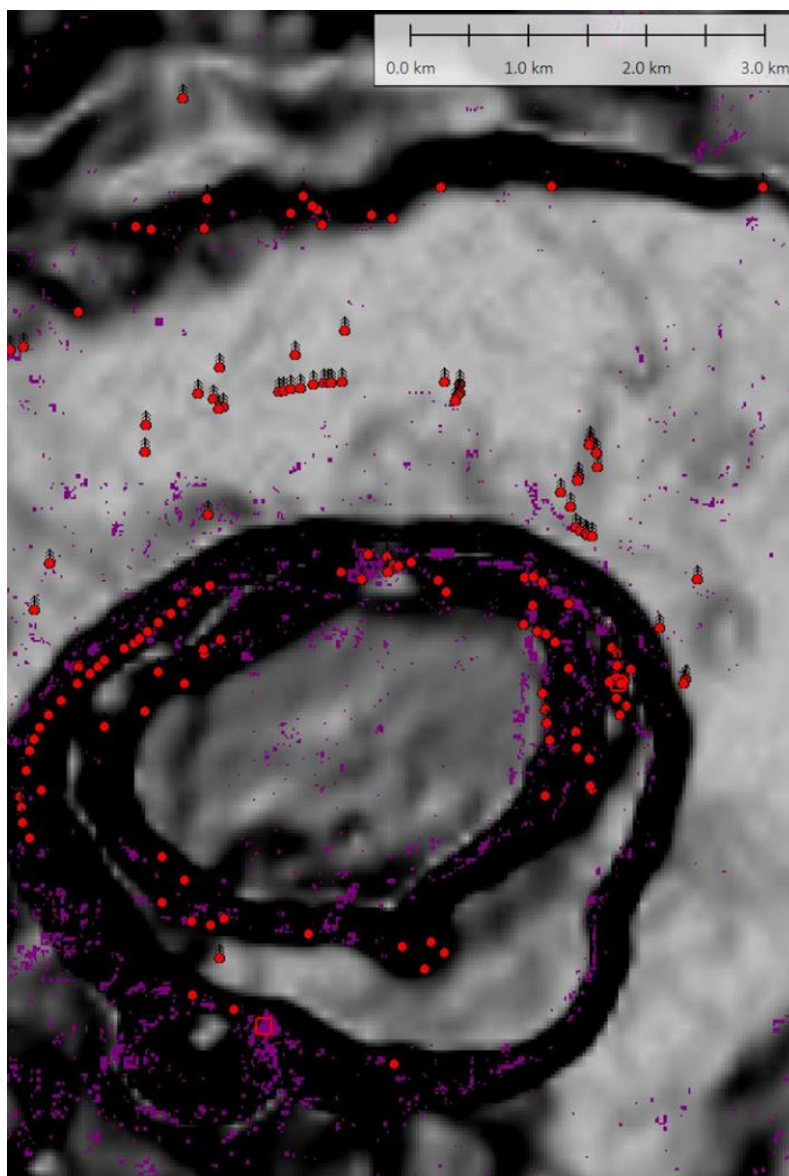


Figure 5: Hillshade of Suswa Caldera Area (from GDC, 2013) with Fumaroles and an ASTER Alteration Class – ASTER classification was based on alteration in small areas of the east and southwest inner caldera and is shown in purple. Note the purple Alteration Class trend immediately west of the fumaroles (red dots with double headed arrows) in the eastern Island Block. Training areas are shown as red rectangles. Some of the alteration class outside of the southwestern inner caldera near Ol Doinyo Nyukie is related to cloud cover in the ASTER scene.

2.2 Geophysics

The EFLA analysis of the geophysical data at Suswa combines the data from several MT-TEM resistivity surveys totaling over 240 MT stations (with 170 generally coincident TEM stations) and two gravity profiles acquired by GDC, along with reviews of earlier geophysical reports and publications including local earthquake monitoring, regional seismic tomography and gravity studies (EFLA, 2017; Cumming, 2018). The main elements of the MT-TEM resistivity interpretation have been illustrated by a representative example of the MT-TEM resistivity maps and cross-sections produced by 1D and 3D inversions, including the map of resistivity at 1500 masl in Figure 9 and the N-S resistivity cross-section in Figure 10. The implications of the local earthquake monitoring for shallow magmatic activity at Suswa are reported in Kipngok et al. (2017). The correlation of the MT-TEM resistivity with the interpreted geology and hydrology and the conceptual implications derived from the resistivity maps and cross-sections are illustrated in the conceptual model section of this report.

In the context of a volcano-hosted geothermal resource, the MT-TEM resistivity pattern is expected to include low resistivity smectite clay alteration that caps the higher resistivity and higher temperature alteration associated with the upflow (Ussher et al., 2000; Árnason et al., 2000). For water dominated reservoirs, the smectite alteration also typically caps peripheral outflows below the water table (Cumming, 2016). However, at Suswa, the MT does not resolve a typical candidate for a capped upflow, probably because the most promising location for an upflow from a geological and geochemical perspective is below the Suswa inner caldera (Figure 10), where MT coverage is sparse because of limited access. Despite these limitations, the MT-TEM provides evidence supporting the interpretation of most of the fumaroles outside the Suswa inner moat as leakage from a steam and condensate outflow at the base of a dense, high resistivity zone, most likely a brittle massive lava flow, an important component of the resource conceptual model.

Although the limited MT coverage over the Central Island could not detect a conventional resistivity pattern associated with a geothermal upflow, the MT over the outer caldera does detect ambiguous evidence of a deep, relatively low resistivity zone (30 to 40 ohm-m) extending north from the inner caldera at below sea level, most reliably at about -1000 m elevation (about 2600 m depth; as represented in a north-south cross section discussed below in the Favored Conceptual Model Section 4, Figures 9 and 10). Because of MT data quality limitations and the limitations of the MT inversion methods, the 1D and 3D MT imaging is not reliable at depths greater than 2600 m at Suswa. However, this pattern of relatively low resistivity below the expected depth range of smectite clay alteration in this geologic context may be correlated with proximity to magma and temperatures over 380°C (Gasperikova et al., 2015). In potentially analogous reservoirs like Menengai in Kenya (Mibei et al., 2016), the conventional production is generally at <350°C and scaling and low permeability have been problematic for production at >350°C.

The color shading of MT resistivity in the N-S cross-section shown in Figure 10 shows a >100 ohm-m (blue) zone at about 1500 masl that is consistent with a lava embedded in volcanic ash and breccia, also supported by the high gravity coincident with this high resistivity feature (EFLA, 2017; Cumming, 2018). The close correlation of the outline of this resistivity feature with the extent of fumaroles (Figure 9) is consistent with the interpretation of steam-condensate being distributed in a basal lava breccia and leaking up faulted zones. The 7 to 50 ohm-m moderate resistivity (shaded green in Figure 10) extends to a depth of about 1000 to 1500 m in the north and to about 1500 to 2000 m in the south and are likely to correspond to pre-Suswa volcanoclastics and sediments with significant clay content, but more illite than smectite. These rocks are likely to be impermeable, forming a lateral seal to the Suswa system. The underlying basement rocks are very resistive, probably much higher resistivity than 100 ohm-m based on measurements on outcrop elsewhere in the East Rift, and they are likely to be impermeable except where intruded by recent volcanic rocks.

Due to the deleterious effect on the 3D MT inversion of the gap in MT coverage over the Suswa inner caldera and also due to limitations of the single-site approach to the acquisition and processing of MT data at Suswa (EFLA, 2017), the MT resistivity patterns were interpreted cautiously; for example, the resistivity in Figure 10 is plotted to <2500 m depth. However, for a subset of relatively well-constrained cross-sections, resistivity plots were produced showing the results of 1D and 3D resistivity inversions to 4500 m depth (Cumming, 2018). Although the analysis suggests that the results of the MT resistivity imaging below about 2500 m depth are not generally reliable, the deeper MT imaging is shown to be compatible with the existence of a <30 ohm-m feature below 3000 m depth, within the outer caldera near the northern margin of the inner caldera. In the geological context of Suswa, this would be consistent with magma as shallow as 3000 m depth.

Lagat and Malimo (2013) and Kipngok et al. (2017) show a pattern of epicenters of small earthquakes at Suswa that, in the context of a volcano with very recent lava eruptions and ongoing deformation indicated by InSAR, suggests that there is episodic movement of magma below the southeast moat of the inner caldera, perhaps an intruding dike or a recently solidified dike being rapidly cooled by cold water down flow. Such evidence suggests the proximity of a high temperature geothermal upflow but also a relatively shallow 400°C isotherm that is likely to limit the thickness (and capacity) of an associated conventional geothermal reservoir since production from zones over 350°C is usually limited. Some risk of eruption is also implied by the seismic activity and InSAR deformation, although this type of activity is common in rift-hosted geothermal prospects over time intervals of a few years, whereas eruptions take place over intervals of centuries.

The overall pattern of the geophysics is consistent with the existence of a very hot geothermal reservoir that has a shallow magmatic heat source, suggested by the earthquake pattern and by ambiguous evidence from a low resistivity zone below -1000 masl. Zones of shallow steam flow appear to be hosted in gently dipping formations like those intersecting the western wall of the inner caldera moat. Although some shallow steam zones are likely to be too thin to be reliably imaged by the MT, a >100 ohm-m resistive zone at about 1300 to 1600 masl is embedded within the moderately conductive rocks north of the inner caldera moat and south of the northern rim of the outer caldera. This resistive feature is spatially correlated with the distribution of fumaroles north of the inner moat and, since the base is close to the expected water table, this is interpreted as a likely lava that hosts a steam-condensate outflow along a basal auto-breccia, leaking steam to the fumaroles where the lava is faulted and around its up-dip edges on the outer caldera rim. Although the limited MT coverage at Suswa does not image a typical low resistivity smectite zone capping a likely upflow, the MT-TEM resistivity pattern is permissive of a geothermal upflow below the Suswa inner caldera.

2.3 Fluid Chemistry

Results of chemical analyses of fumarole samples were used to characterize the origin of the fluids as well as the physicochemical properties of the geothermal reservoir present in Suswa. Maps of the CO₂/H₂S gas ratio and the helium isotope ratio (³He/⁴He) and a trilinear diagram of helium (He), argon (Ar), and nitrogen (N₂) shown in Figure 6 suggest that the fumarolic steam discharged within the inner caldera has less air contamination and a stronger magmatic component than those from the outer caldera. The noble gas data also indicates that there is a magmatic component to the gas discharged in the eastern and western moat, that is, the ³He/⁴He ratios in fumaroles SWF-8 and SWF-3 are magmatic whereas the source of noble gases in the rest of the fumaroles is air. Gas geothermometers applied to fumaroles within the moat indicate a wide range of reservoir temperatures (250 to 350°C), but the more reliable geothermometers (those based on ratios without air-related gases; CO₂-H₂, H₂S-CO₂) suggest a temperature range of 250°C to 295°C. Therefore, the gases provide evidence for two upflow zones or two permeable paths to the surface from a common system: one in the eastern moat in the vicinity of SWF-8 and one in the south western moat in the vicinity of SWF-3.

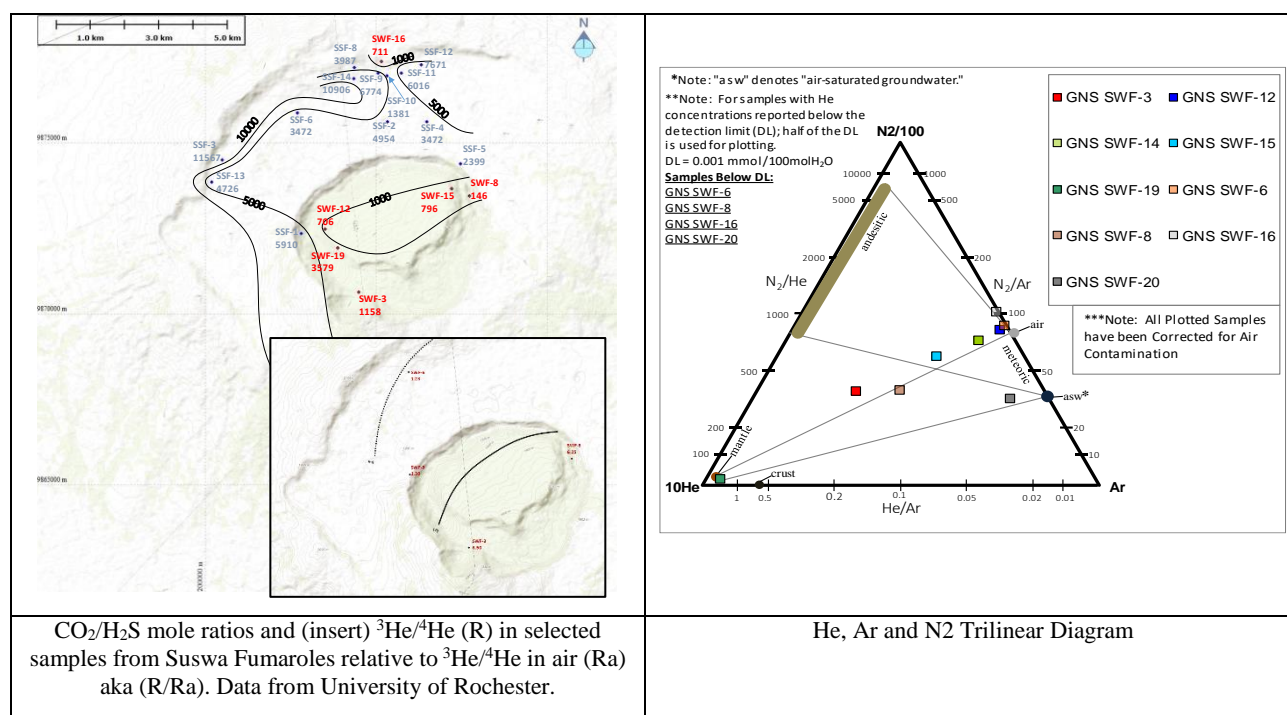


Figure 6: Distribution of CO₂/H₂S, helium isotope (³He/⁴He) ratios and relative concentrations of helium (He), argon (Ar), and nitrogen (N₂) (trilinear diagram)

Combining gas geothermometers and stable isotopes (Figure 7Figure 7), the fumarole chemistry suggests that the fumarole steam is probably derived from local meteoric water as sampled east of the project area. The water is heated to 220 to 260°C by deep circulation with some relatively minor positive shift in $\delta^{18}\text{O}$, then possibly boiled at relatively high temperatures (220 to 300°C) creating a reservoir vapor zone. Another alternative is that the source of the reservoir liquid is more distant and isotopically heavier, so that the water heats and circulates upward then boils near the water table at 100°C. The pattern of stable isotopes of steam condensate and the lower $\text{CO}_2/\text{H}_2\text{S}$ ratios indicate that the steam closest to the upflow occurs in the western and eastern moats of the inner caldera. Isotopic and gas/ratio data suggest that the steam discharging on the outer caldera floor and rim to the north and south of the inner caldera could be the result of partial condensation, with or without mixing with higher elevation (relative to the sampled water east of the project area) meteoric water. The results are consistent with boiling in the upflow zones at Suswa at high temperatures ranging from 250 to 300°C, or that Suswa geothermal system is possibly vapor dominated or at least two-phase in the reservoir.

3. CONCEPTUAL MODEL

3.1 Heat Source

The Suswa hydrothermal system expresses magmatic heat evident in high helium isotope ratios and the co-location of concentrated young volcanic and fumarolic activity in the calderas of Suswa Volcano. The recent, frequent, and voluminous volcanic products, re-collapsed and resurgent calderas shown in Figure 2, tectonic setting, and volcanic rock petrology suggest that the Suswa magmatic heat source occurs as a multiphase intrusive complex with persistent magma residence over long periods through the later life of the volcano. Petrology of the volcanic rocks records magma mixing based on zoning and resorption of phenocrysts suggesting periodic renewal of the magma (Espejel-Garcia, 2009). Meanwhile the lack of recent mafic volcanic rocks is consistent with the formation of a shadow zone formed by a persistent, relatively low density phonolitic magma at depth. In contrast at Silali Caldera, northern Kenya, recent basalts cut across the volcano and young caldera.

Magma were emplaced at various depths. Petrologic studies by White et al. (2012) estimated that fractionation of Suswa trachyte from basalt occurred at 14 km depth. Deep high seismic velocity interpreted from seismic studies (Simyu and Keller, 2001) at about 5 km depth along the rift may represent crystalline intrusive rock related to long term persistent deep dike. A low resistivity zone may occur at about 3 km depth in MT resistivity cross-sections (Cumming, 2018). In contrast, the fractionation depth for the Olkaria Rhyolite, about 30 km to the NNW of Suswa, was estimated to be 3.5 km.

Subsidence patterns measured from satellite radar interferometry were interpreted to reflect deflation at depths of 2.5 to 5 km below the inner caldera (Biggs, 2009) possibly due to active magma movement. A model of a subsiding or cooling magmatic sill would put the source close to the 2.5 km depth estimate. A more plug-shaped intrusion would be deeper. The 5 km depth estimate is based on a geologically unreasonable point source. A liquid magma may dominate the highest reservoir temperatures. Caldera unrest studies (e.g. Waite and Smith, 2002) suggest that release of over-pressured hot water can also cause caldera subsidence.

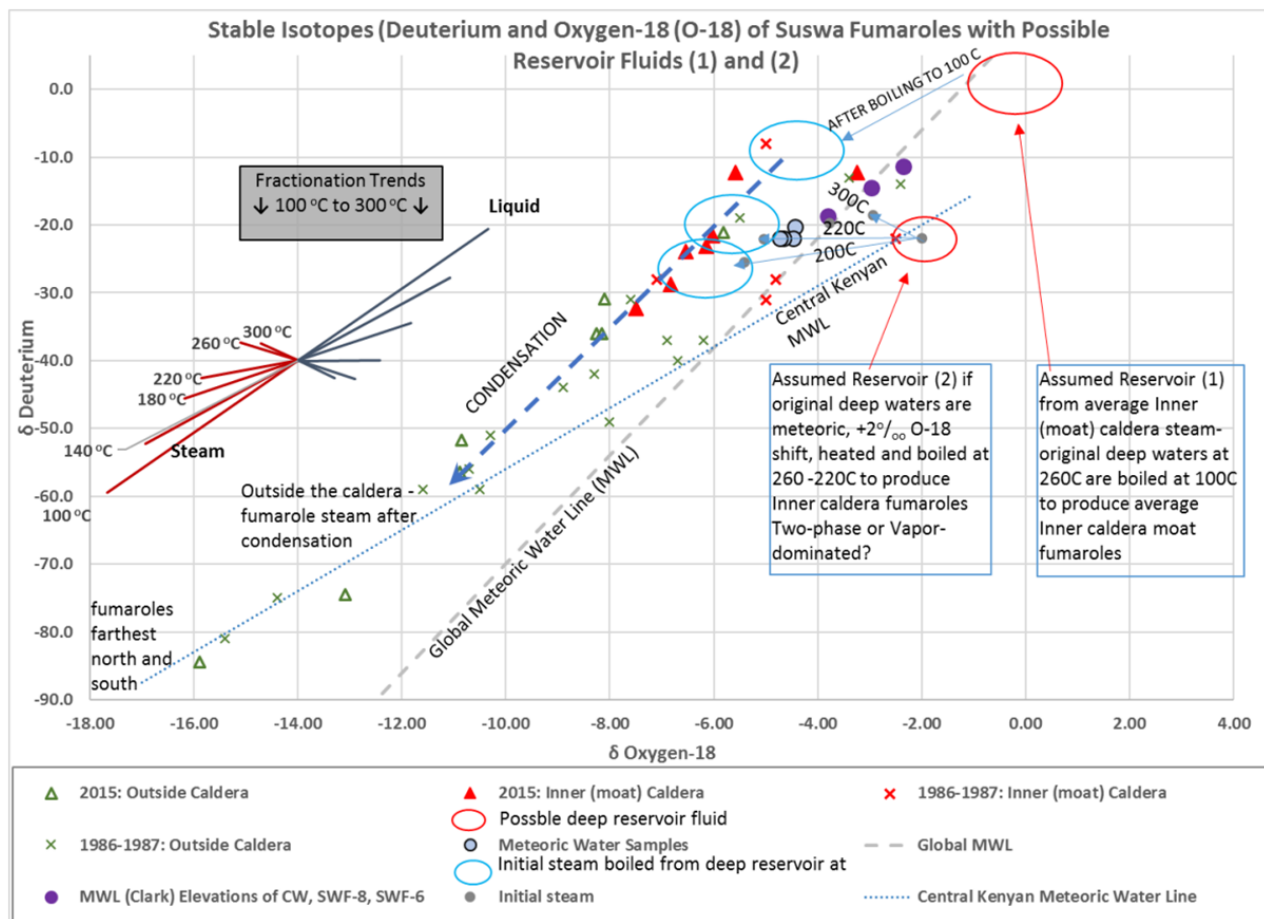


Figure 7: Oxygen-18 and deuterium of fumarolic steam and local meteoric waters. Isotopic composition of fumarolic steam from the inner caldera could be generated in two ways, 1) meteoric water, with a typical oxygen-18 shift of 2mil and then boils at 220 to 260°C, or 2) inner caldera steam is derived from isotopically heavier 260°C reservoir liquid boiled at 100 °C. The steam condenses and possibly mixes with meteoric water forming fumaroles farthest north and south of the caldera.

Seismicity maps (Kipngok et al., 2017) suggest that recent magma may be focused under the SW inner caldera margin near the Ol Doi Nyukie volcano (Figure 2). An alternative model for the seismicity suggests that cold downflow from rainfall on Ol Doi Nyukie is invading along the inner caldera ring fault into very hot rock above and in the upper solidified interior portions of a shallow intrusion. In this case, the seismicity would represent cooling-induced rock fracturing driven by tectonic and magmatic stresses. In both cases, the reservoir in this local area may be limited, either by very high temperature impermeable rock or by permeable but rapidly cooling rock.

The likely magma cooling rate suggests that Suswa volcano is currently underlain by high temperature volcanic rock focused below the inner caldera but extending below the outer caldera. The cooling time for a simple 1 km thick shallow sill should range from about 5,000 to 50,000 years depending on water convection patterns and surrounding rock temperature (Cathles, 1981). Heat from a single intrusive event of moderate size like this might support a hydrothermal system for a few tens of thousands of years (Cathles et al., 1997). After formation of the outer caldera at Suswa, five significant intrusive events related to eruptions of lava, Ol Doi Nyukie volcano, inner caldera collapse and resurgence, and post resurgence lavas have occurred in the last 100 ka, possibly resulting in multiple overlapping phases of hydrothermal activity.

3.2 Permeability and Geomechanics

Evidence for permeability from structural geology at Suswa is dominated by two controlling factors, rift-caldera fault interactions and tuff stratigraphy. Regarding general stratigraphy, the combination of weak tuffs and stronger lavas and sills in the shallow section is likely to lead to numerous fractures associated with the differing mechanical responses to deformation between the lavas and tuffs, this may lead to stratigraphically controlled fracture zones especially along faults in the relatively young lava-tuff sequence. Meanwhile deeper parts of the volcanic section are not reported to have tuff beds but have had a longer history of faulting and may be more extensively broken. In this zone fracture patterns may be steeply dipping.

Fumaroles aligned with tuff outcrops in the northwest inner caldera scarp (Figure 4) suggest that the tuff is broadly permeable, and lavas are impermeable. This pattern of fumarole alignment also occurs in the caldera wall at Silali in another tuff interbedded with lava. Exploration elsewhere suggests that tuff permeability is not strongly evident in hydrothermal systems where tuffs form thick accumulations or where they alter to impermeable clays at temperature under about 180°C. Permeability in tuffs at Suswa may be related to the interaction of fractures with interbedded tuff and lava and, at lower temperature, perhaps enhanced by a tendency of phonolite and trachyte tuffs at Suswa to resist alteration to smectite clay above the water table (Cumming, 2016).

Fault irregularities are important for understanding fluid flow. Generally, fault irregularity types include fault tips, intersections, bends, step-overs, ramps, and accommodation zones. At Suswa, a number of fumaroles occur near fault irregularities that may create permeability that penetrate the hydrothermal cap. A worldwide study showed that locked fault irregularities in various tectonic settings dominate fracture permeability open to hydrothermal flow, including in magmatically heated areas (Curewitz and Karson, 1997). Examples of locking include fault tips, fault intersections with incompatible movement on the two faults, or fault bends where fault movement is across the bend (e.g., Figure 8).

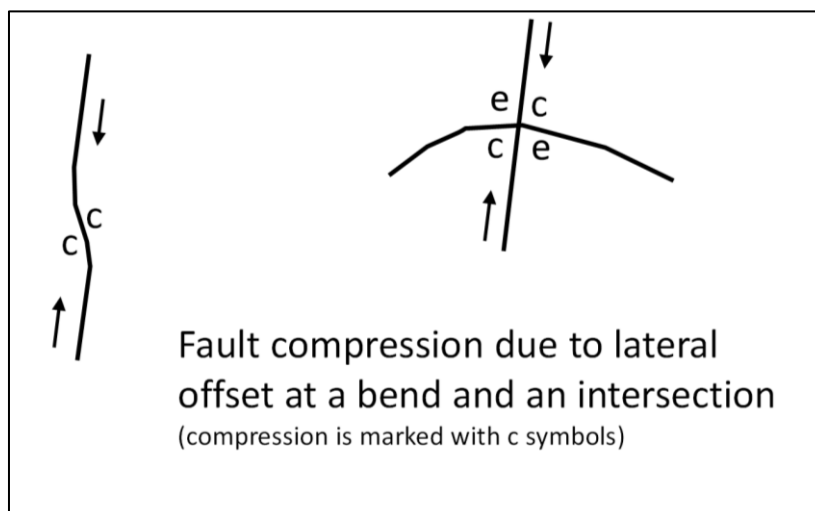


Figure 8: Simplistic Stress Interpretations on Oblique Rift-Caldera Fault Intersections and at a Constraining Bend in a Right Lateral Fault (from Melosh, 2017) – The symbol “c” refers to compression while “e” refers to extension. A slight counterclockwise rotation of this figure would make it applicable faults shown in Figure 2.

Mapped patterns of likely permeability are interpreted from mapped alteration, fumaroles, and gas chemistry along with fault irregularities and the distribution of rock formations. Permeability is interpreted to extend to greater depth near fumaroles with high temperature gas chemistry and near alteration with sulfur deposition or abundant silica (both latter cases are based on inferences regarding high temperature gas chemistry in steam).

Structural complexities such as fault irregularities and intersections in the eastern inner caldera and moat and in the southwest caldera coincide with densely spaced fumarolic activity. In these areas, right-lateral transverse rift faults intersect the caldera rim structure producing extensional stress (Figure 3) and potential permeability. Other areas with evidence of structural permeability that is less compelling include the northern rim of the outer caldera and the northern moat between the inner and outer calderas.

Beyond the suggestion of potential reservoir permeability based on fumarole chemistry, the actual depth extent of permeability is unknown. Generally, the permeability related to a specific fault irregularity is likely to decline with depth, although the number of fractures may increase due to the longer history of faulting in older rocks. Meanwhile an underlying magma and its contact metamorphic halo generally limit conventional production to under 380°C and typical production to under 350°C. Given these likely limits and the evidence of magma from the geology and geophysics at Suswa, below about 2.5 km depth, targeting reservoir permeability will be increasingly risky.

3.3 Cap Rocks and Low Permeability Seals

Because of the paucity of MT-TEM stations within the inner caldera, the Suswa resistivity imaging does not detect an extensive low resistivity geothermal cap rock pattern similar to those at potentially analogous geothermal fields (EFLA, 2016). However outside of the inner caldera thick moderately low resistivity may represent moderately low to low permeability altered rock that seals the lateral margins of the reservoir in the inner caldera and caps a possible deep outflow to the north. The base of the reservoir may be formed by a low permeability contact metamorphic zone above a magma or just rapidly declining permeability due to overburden compression.

The extensive fumarolic activity above the inner caldera margins and in faulted trends of young lava flows below the northern outer caldera moat and the Island Block suggest that these lavas may act as aquicludes where they are not broken when emplaced or subsequently faulted. An alternate interpretation that the fumarole pattern is related to high permeability of fractures in the lava that elsewhere are rapidly resealed in weaker tuffs is not consistent with the numerous fumaroles that produce from tuffs. The number of fumaroles with possible groundwater interaction reveals that the cap (perhaps like others in Kenya) is relatively leaky compared to fields where fumaroles are much less abundant. It has been proposed that because of its mineralogy, trachyte rocks are less likely to form smectite, perhaps accounting for the permeability of tuffs at shallow depth at Suswa.

3.4 Recharge

Groundwater in the rift valley is dominated by regional flow of meteoric water from above the rift scarps to the east and west and then down the rift toward lower elevations to the south beyond Suswa Volcano. The regional water table is expected to be about 500 m depth (1200 m elevation) below the volcano. Significant local rainfall also occurs, including about 75 cm/year at the town of Suswa at 1600 m elevation (www.Climate-data.org). Rainfall at higher elevations on the volcano, such as Ol Doiyo Nyukie at 2200 m elevation, is expected to be stronger (Davies et al., 1985).

Recharge to the reservoir is likely to be from a combination of cold local meteoric and hotter, deeper regional sources. Downflow of local meteoric water is expected to encounter what may be a discontinuous clay cap and stratigraphic lava flow barriers where the water can perch at shallow depths before finding vertical fracture conduits near faults and intersections that might deliver water to the reservoir. Recent eruption vents and fissures may also provide a path for cold water to enter the subsurface and encroach on the top of the geothermal reservoir, as it has at Menengai in Kenya (Mibei et al., 2016). In such cases cold meteoric downflow may penetrate more deeply to quench the reservoir locally. Regional water recharge is probably deeper and hotter.

The broad expression of condensation interpreted from steam isotopes and CO₂/H₂S ratios is consistent with cooling increasing away from the inner caldera. Condensation could also be related to cooling from the influx of meteoric water, probably flowing down from the surface, interacting (yet not fully quenching) the steam across broad areas in the shallow steam zone north and south of the main upflow. Abundant fumarole occurrence and limited evidence for an intensely altered clay cap, especially within the inner caldera, suggests that cold meteoric water is likely to encounter permeable avenues down through the combined lithologic and alteration cap. Permeable areas without fumaroles near fault intersections are candidates for cold water downflow.

This aspect of the conceptual model is suggested by similarities with evidence for cold invasion at Menengai (Mibei et al., 2016). Another useful analog for multiple recharge waters such as those proposed here occurs at the Puna Geothermal Field along the East Rift Zone on Kilauea Volcano in Hawaii. Water chemistry from long term flow tests showed contributions from both meteoric water and sea water in the reservoir.

3.5 Flow Patterns

The two primary sources of fluid flow are interpreted to be geothermal upflow below the inner caldera and lateral meteoric recharge from the north along the rift at depth. Meteoric input flowing vertically down from the surface of the volcano is expected to be lower volume but locally important. Flow patterns are indicated by arrows in the model drawing (Figures 9 and 10).

Geothermal upflow in the inner caldera may occur along stressed fault irregularities in a fracture network that includes the ring faults of the inner caldera and Island Block. The best candidates for deep upflow are identified at the surface based on fault patterns and fumarole chemistry at the east end of the Island Block and in the SW inner caldera moat. A breach in the cap along the inner caldera ring fault may also allow local downflow.

In the favored model reservoir steam from the inner caldera flows to the north and south along the rift axis faults and in stratigraphic traps at about 100°C at the top of the interpreted water level. This configuration based on the strongly expressed condensation trend evident in the gas chemistry, the interpreted water table, and the buried lava flow resistor in the outer caldera that correlates with the fumarole occurrence. To the south, shallow resistors are thin and much less extensive and fumarole activity is limited.

An upside alternate model includes high temperature outflow at deeper levels to the north or a separate upflow on the northern outer caldera ring fault.

4. FAVORED CONCEPTUAL MODEL

Long term, repeated intrusion and residence of magmas at Suswa has delivered heat to a large area at depth focused on the Suswa caldera complex and extending along the axis of the rift to the north and south. Renewed magma emplacement recently occurred below the inner caldera providing intense localized heat. Fracture networks have developed, especially below the inner caldera moat due to repeated magmatic and tectonic movements including competing offsets on concentric ring fractures around the inner caldera and the Island Block and cross-cutting right lateral-normal rift faults. Hydrothermal circulation at depth below the inner caldera in these networks developed a mature geothermal circulating system that has established commercial temperatures, interconnected permeability, and chemical and mineralogic geothermal equilibrium in a reservoir somewhere between 500 and 2500 m depth in the inner caldera. Deep permeability is localized near specific fault interactions and extends along the inner caldera ring fault zones and below the Island Block. Reservoir cap seals may be associated with clay alteration, lava flows or veins deposited due to boiling at the top of the reservoir. The lateral boundaries around the inner caldera may include low permeability in moderately altered volcanic rock subject to fracture compression outside the inner caldera and outer calderas.

Recharge water is dominated by regional groundwater flow along the valley from the north originating in rainfall on the highlands above the east and west rift scarps. Recharge patterns also include local downward flow of meteoric water from nearby high elevation sources.

In addition to the two fumarole areas in the eastern and southwestern inner caldera that deliver gases to the surface that are consistent with a 250 to 300°C geothermal reservoir, there are abundant steam emissions elsewhere in the inner and northern outer caldera that are progressively modified by condensation in shallow outflows to the north and south. The extensive condensation suggests cooling to about 100°C during outflow near the top of the interpreted water table at about 500 m depth below a buried lava flow. The condensation strips soluble gases and heavy isotopes from the steam. This outflow may represent the waning stage of a previously hotter outflow as suggested by areas of intense sulfurous alteration on the northern and northwestern outer caldera rim and at the southern fumaroles.

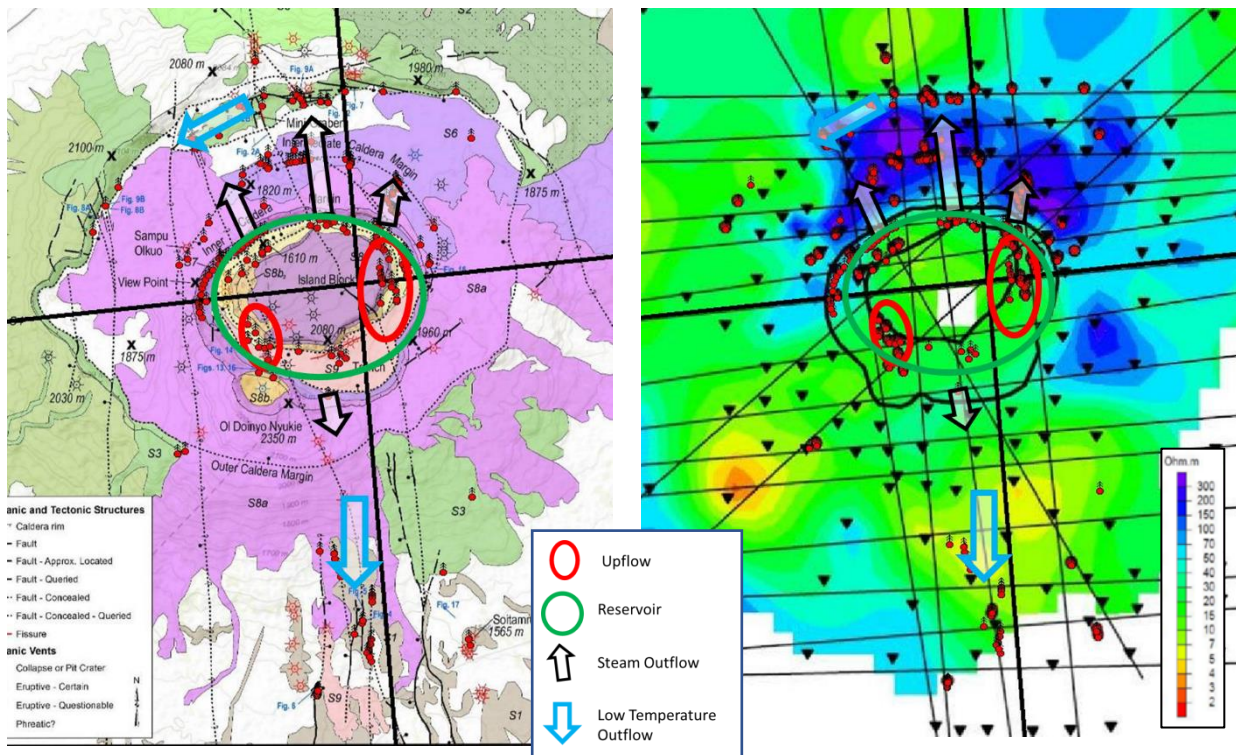


Figure 9: Left: Suswa Caldera Conceptual Model Map (reduced in scale from Figure 2) – Upflow, reservoir, and outflow patterns are from the favored model. Bold lines show the traces of the NS and WE model cross-sections. For the complete legend and scale of the original map refer to Figure 2. Right: MT Resistivity at 1500 masl overlain with Conceptual Model Flow Patterns (EFLA, 2017). The buried resistor north of the inner caldera correlates with most of the fumaroles (symbol ⬆) in the outer caldera. Both Left and Right figures cover the same area.

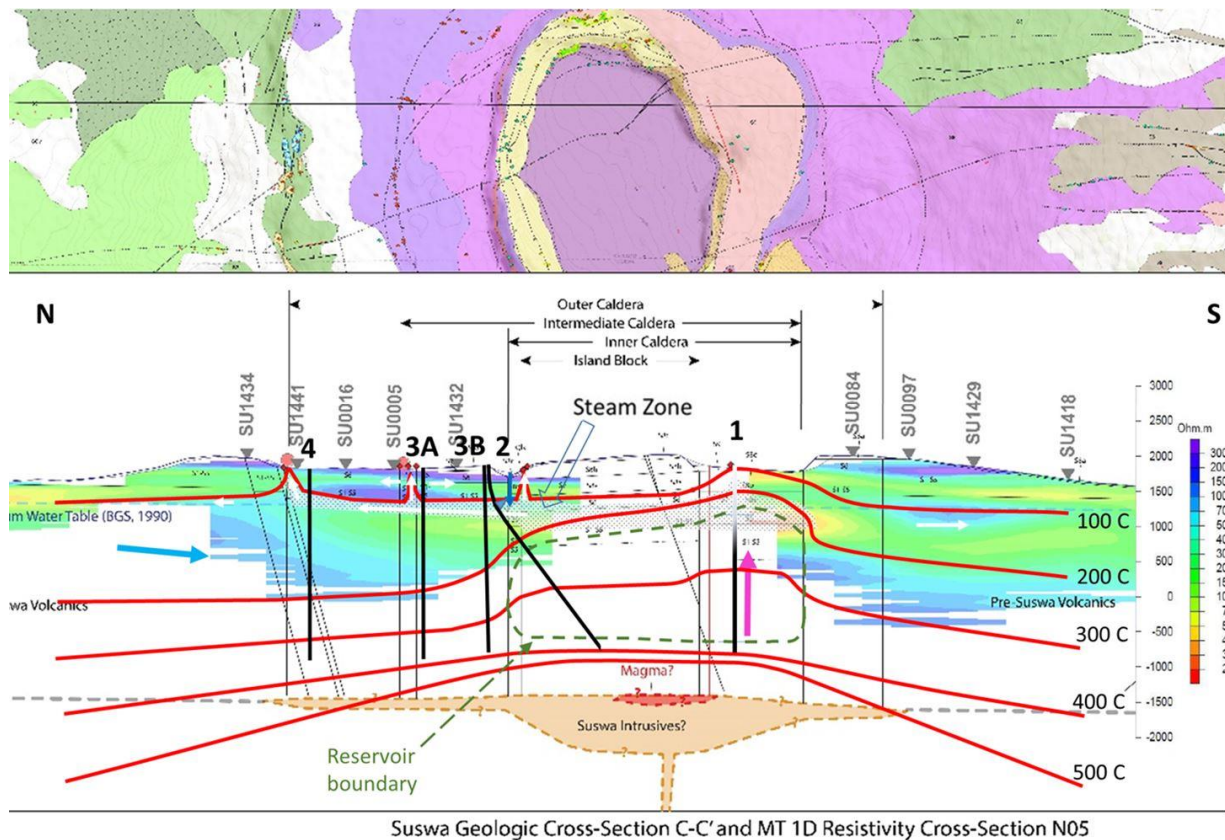


Figure 10: N-S Cross-Section with Favored Conceptual Model (EFLA, 2016) – Upflow occurs on the eastern rift-ring fault zone intersection, reservoir extends under the Island Block Cap (green dashed line), and a shallow steam outflow flows north below a buried lava cap at the top of the water level. The base of the reservoir is controlled by a sill at about 2.5 km. No vertical exaggeration. This section line is shown at scale in Figure 2.

4.1 Model Alternatives

In order to accommodate the data, analysis and conceptual interpretation uncertainties noted in the technical discussion, the properties and extent of elements of the conceptual model have been varied in the resource assessment. The principal variations are as follows:

1. Upside: Deep, high temperature outflow to the north below the thick moderately low resistivity altered cap below the outer caldera moat may rise from 2 km to about 1 km depth at intersections and in fault ramps along the northern outer caldera ring fault-normal fault zone. In this case, there would be a deep and relatively hot reservoir under the northern outer caldera along the rift beneath the shallow 100°C condensing aquifer.
2. Downside: The high temperature reservoir may be invaded by cold influx along the inner caldera ring fault zone or through recent eruption vents, for example, from Ol Doinyo Nyukie or the Island Block. Cold influx would limit the volume of the reservoir in the inner caldera.
3. Downside: Magma shallower than 3 km depth would curtail the expected thickness (and volume) of the producible resource. Magma is likely at 2.5 to 5 km depth based on several lines of evidence, especially below the SW inner caldera.

CONCLUSIONS

Integrated geologic, geochemical and geophysical investigations successfully constrained a reasonable range of conceptual models for the Suswa Volcano geothermal system. The preferred model includes:

- A magmatic heat source is likely to be found at 2.5 to 5 km depth in part of the prospective area.
- A 250 to 300°C liquid reservoir overlain by a two-phase zone extends below parts of the ring fault zone and Island Block- and possibly throughout the inner caldera
- Extensional fault complexities and coincident leakage of deep fluids characterize a likely neutral and permeable high temperature reservoir.
- Based on the combined fumarole chemistry and structure, the reservoir upflow would be expected at the east and west ends of the Island Block
- A 100°C outflow is likely hosted below a buried lava, just above the water table, in the northern outer caldera. A similar outflow may extend to the south.

REFERENCES

- Achauer, U., Maguire, P.K.H., Mechie, J., Green, W.V., and the KRISP Working Group, 1992. Some remarks on the structure and geodynamics of the Kenya Rift: *Tectonophysics*, no. 213, p. 257-268.
- Atmaoui, N., and Hollnack, D., 2003. Neotectonics and extension direction of the southern Kenya rift, Lake Magadi area: *Tectonophysics*, no. 364, p. 71-83.
- Ármannsson, H., 1987. Studies on the geochemistry of steam in the Suswa and Longonot areas and water in the lake Magadi, Kedong valley and Lake Turkana areas, Rift valley Kenya: Technical report KEN/82/002 - Exploration for geothermal energy. Department of Technical Cooperation for Development, United Nations, Nairobi.
- Árnason, K., Karlsdóttir, R., Eysteinnsson, H., Flóvenz, Ó., and Guðlaugsson, S., 2000. The resistivity structure of high-temperature geothermal systems in Iceland. In: *Proceedings of the 2000 World Geothermal Congress*, Tohoku-Kyushu, Japan, 923-928.
- Baker, B.H., Mitchell, J.G., and Williams, A.J., 1988. Stratigraphy, geochronology and volcano-tectonic evolution of the Kedong-Naivasha-Kinangop region, Gregory Rift Valley, Kenya: *Journal of the Geological Society*, London, v. 145, p. 107-116.
- BGS, 1990. Geological, volcanological and hydrogeological controls on the occurrence of geothermal activity in the area surrounding Lake Naivasha, Kenya: Republic of Kenya, Ministry of Energy, 138 p.
- Biggs, J., Anthony, E.Y., and Ebinger, C.J., 2009. Multiple inflation and deflation events at Kenyan volcanoes, East African Rift: *Geology*, v. 37, no. 11, p. 979-982.
- Bonavia, F.F., Chorowicz, J., and Collet, B., 1995. Have wet and dry Precambrian crust largely governed Cenozoic intraplate magmatism from Arabia to east Africa?: *Geophysical Research Letters*, v. 22, no. 17, p. 2337-2340.
- Bosworth, W., Strecker, M.R., and Blisniuk, P.M., 1992. Integration of east African paleostress and present-day stress data: Implications for continental stress field dynamics: *Journal of Geophysical Research Letters*, v. 97, no. B8, p. 11, 8851-11,865.
- Cathles, L. M., 1981. Fluid flow and genesis of hydrothermal ore deposits. In: Skinner, B.J. (ed.), *Economic Geology: 75th anniversary volume*, pp. 424-457.
- Chorowicz, J., Collet, B., Bonavia, F.F., and Korme, T., 1994. Northwest to north-northwest extension direction in the Ethiopian rift reduced from the orientation of extension structures and fault-slip analysis: *Geological Society of America Bulletin*, v. 105, p. 1560-1570.
- Chorowicz, J., 2005. The East African rift system: *Journal of African Earth Science*, v. 43, p. 379-410.
- Cumming, W., 2016. Resource conceptual models of volcano-hosted geothermal reservoirs for exploration well targeting and resource capacity assessment: construction, pitfalls and challenges: *Geothermal Resources Council Transactions* 40, 623-638.
- Cumming, W., 2017. Geophysical Section, Review of the Conceptual Model of Suswa Geothermal Prospect, Kenya: Supplement to GDC dated 27-Apr-2017 on: EFLA, 2016. Review of the Conceptual Model of Suswa Geothermal Prospect, Kenya. Final

- Report by EFLA Consulting Engineers to the Icelandic Development Agency/Ministry of Foreign Affairs Project ICE23066-1301NDF Kenya/1 NDF:C48, 2017.
- Curewitz, D. and Karson J. 1997. Structural Settings of Hydrothermal Outflow: Fracture Permeability Maintained by Fault Propagation and Interaction” Jour. of Volc. And Geothermal Research, 1997, 79, pp. 149-168
- Davies, T., C. Vincent, and A. Beresford, 1985. July-August Rainfall in West-Central Kenya: J. Climatology, Vol. 5, 17-33.
- Delvaux, D., and Barth, A., 2010. African stress pattern from formal inversion of focal mechanism data: Tectonophysics, no. 482, p. 105-128.
- EFLA, 2016. Review of the Conceptual Model of Suswa Geothermal Prospect, Kenya: Final Report by EFLA Consulting Engineers to the Icelandic Development Agency/Ministry of Foreign Affairs Project ICE23066-1301NDF Kenya/1 NDF:C48, 2017.
- Espejel-Garcia, V.V., 2009. Suswa volcano, Kenya rift: Evidence of magma mixing, sodium-fluorine complexing and eruptions triggered by recharge: Ph.D. thesis, El Paso, University of Texas, 113 p.
- Gasperikova, E., Rosenkjaer, G., Árnason, A., Lindsey, N., 2015. Resistivity characterization of the Krafla and Hengill geothermal fields through 3D MT inverse modeling: Geothermics 57. DOI: 10.1016/j.geothermics.2015.06.015
- GDC, 2013. Feasibility report for exploration and appraisal drilling in Suswa geothermal prospect: Internal GDC Report.
- Hinz, N., 2017. Geology Section, Review of the Conceptual Model of Suswa Geothermal Prospect, Kenya: Supplement to GDC dated 12-Mar-2017 on: EFLA, 2016. Review of the Conceptual Model of Suswa Geothermal Prospect, Kenya. Final Report by EFLA Consulting Engineers to the Icelandic Development Agency/Ministry of Foreign Affairs Project ICE23066-1301NDF Kenya/1 NDF:C48, 2017.
- Johnson, R.W., 1969. Volcanic geology of Mount Suswa, Kenya: Philosophical Transactions of the Royal Society of London, Series A., Mathematical and Physical Sciences, v. 265, no. 1164, p. 383-412.
- Kipngok, J., Magnússon, R., Melosh, G., Haizlip, J., Cumming, W., Hinz, N., Harvey, M., Alexander, K., Lopeyok T., Mwakirani, R., Wamalwa, A.M., Malimo, S.J., and Auko, L.O., 2017. Geothermal Conceptual Model of Suswa Volcano, Kenya: Geothermal Resources Council Transactions 40.
- KPC, 1993. Draft report of surface manifestations of Suswa geothermal prospect: KPC Report. 113 p.
- Lagat, J.L. and Malimo, S.J., 2013. Suswa Geothermal Prospect: Feasibility Report for Exploration and Appraisal Drilling: *GDC Internal Report*, 99 p.
- MacDonald, R., Kjarsgaard, B. A., Skilling, I. P., Davies, G. R., Hamilton, D. I., Black S., 1993. Liquid immiscibility between trachyte and carbonate in ash flow tuffs from Kenya: *Contributions to Mineralogy and Petrology*, **114**, p 276-287.
- McCall, G.J.H. and Bristow, C.M., 1965. An introductory account of Suswa volcano: *Bulletin Volcanologique*, v. **28**, p. 333-367.
- Melosh, G., 2017. Conceptual Model Section, Review of the Conceptual Model of Suswa Geothermal Prospect, Kenya: In: Magnusson, Melosh, Haizlip, Cumming, Hinz and Harvey, Conceptual Model Review of Suswa – Final Report. by EFLA Consulting Engineers report to the Icelandic Development Agency/Ministry of Foreign Affairs Project ICE23066-1301NDF Kenya/1 NDF:C48, 2017.
- Mibei, G., Mutua, J., Njue, L., and Ndongoli, C., 2016. Conceptual Model of the Menengai Geothermal Field. Proceedings, 6th African Rift Geothermal Conference.
- Mohamud, Y., 2013. 1D joint inversion of TEM and MT data: Suswa geothermal field, Rift Valley, Kenya. Report 19 in: Geothermal training in Iceland 2013. UNU-GTP, Iceland, 411-442.
- Nash, W.P., Carmichael, I.S.E., and Johnson, R.W., 1969. The mineralogy and petrology of Mount Suswa, Kenya: *Journal of Petrology*, v. **10**, p. 409-439.
- Omenda, P.A., 1993. Geological investigations of Suswa geothermal prospect, Kenya: *KPC Internal Report*, 35 pp.
- Randel, R.P., and Johnson, R.W., 1970. Geological map of Suswa area. Degree sheet no. 51, northeast quarter: Kenya Mines and Geology Department, scale 1:125,000.
- Sekento, L.R. and Kipngok, J.K., 2013. Geochemistry of Suswa geothermal prospect: *GDC Internal Report*.
- Simyu, S. and Keller G., 2001. An Integrated Geophysical Analysis of the Upper Crust of the Southern Kenya Rift: *Geophys. J. Intl.*; Vol. 147, Issue 3, pp. 543-561
- Skilling, I.P., 1988. The geological evolution of Suswa volcano, Kenya: University of Lancaster [Ph.D. thesis]: University of Lancaster.
- Skilling, I.P.: Incremental caldera collapse of Suswa volcano, Gregory Rift Valley, Kenya. *Journal of The Geological Society*, London, **150**, (1993), 885-896.
- Smith, M., and Mosley, P., 1993. Crustal heterogeneity and basement influence on the development of the Kenya Rift, East Africa: *Tectonics*, v. 12, no. 2, p. 591-606.
- Strecker, M.R., Blisniuk, P.M., and Eisbacher, G.H., 1990. Rotation of extension direction in the central Kenya Rift: *Geology*, v. 18, p. 299-302.

- Torfason, H., 1987. Geothermal and geological survey of Mt. Suswa, Kenya: Report prepared by the United Nations in cooperation with the government of Kenya for a project of the United Nations Development Programme, 122 p
- Ussher, G., Harvey, C., Johnstone, R., and Anderson, E., 2000. Understanding the resistivities observed in geothermal systems. World Geothermal Congress Proceeds 2000.
- Waite, G., and Smith R., 2002. Seismic evidence for fluid migration accompanying subsidence of the Yellowstone caldera: JGR, Vol. 107, 2002, Issue B9, pp. ESE 1-1–ESE 1-15
- White, J.C., Espejel-Garcia, V.V., Anthony, E.Y., and Omenda, P., 2012. Open system evolution of per alkaline trachyte and phonolite from Suswa volcano, Kenya rift: Lithos, v. 152, p. 84-104.